The Green Valley: Separating Galaxy Populations in Color-Magnitude Space

Undergraduate Research Thesis

Presented in Partial Fulfillment of the Requirements for graduation "with Honors Research Distinction in Astronomy and Astrophysics" in the undergraduate colleges of The Ohio State University

By
Derrick James

The Ohio State University
May 2017

Project Advisor: Dr. Barbara Ryden, Department of Astronomy

Abstract:

Luminous galaxies can be classified as one of two types: early type and late type. Early type galaxies are primarily quiescent ellipsoids, while late types are disk galaxies with active star formation. The differences between these two types create a bimodality in the Color-Magnitude distribution of galaxies. The two populations have a nontrivial region of overlap between them, termed the Green Valley, through which past attempts have been made to place a quantitative divider that splits the two populations on the basis of color. Pulling from the most recent data release of the Sloan Digital Sky Survey, this study seeks to improve upon these attempts by using a larger sample size (particularly at high luminosities), and by considering morphology and spectral information. The spectra of galaxies can tell us whether there has been recent star formation, and whether the galaxy's central black hole is actively accreting matter (known as an Active Galactic Nucleus, or AGN). The populations were separated on these bases, as well as color, and using mathematical modeling and statistical fitting methods, we were able to find an effective divider in each case. The resulting dividers help us probe galactic populations within the Green Valley, specifically those galaxies which contain an AGN.

1. Introduction:

Luminous galaxies can broadly be classified as one of two types: early type and late type. Though the terms are purely conventional, left over from an early (and incorrect) theory of galaxy formation, these two types are quite different from one another. Late type galaxies are generally bluer in color than their early type counterparts, primarily due to the presence of hot, young, massive stars classified by astronomers as O-type and B-type. The color of light is directly related to the temperature of the material, and since hotter matter emits bluer light, these massive stars contribute a lot of blue light to the stellar population. However, these stars are very short lived, with a lifetime on the order of 100 million years, so the presence of these stars indicates that there has been recent (~100 Myr) star formation. Early type galaxies, by contrast, have not had recent star formation, and appear much redder due to the dearth of these O and B stars.

The two types of galaxies differ in more than just color. Late type galaxies generally contain much more gas and dust than do early types. The presence of gas is closely linked to star formation, as dense molecular clouds are necessary to create new stars. The dust can lead to extinction effects on the light emitted by the galaxy. Late types and early types also exhibit morphological differences. Late type galaxies are generally disks with a central bulge (the less luminous ones can be irregular in shape), while early type galaxies have a more tri-axial, ellipsoidal shape. In addition, their surface brightness profiles are described differently. Late type galaxies, if they are disk-dominated (as opposed to bulge-dominated), have light profiles that are

well fit by an exponential: $\log I \propto -r$. Early type galaxies are more centrally concentrated, and are better described by a de Vaucouleurs profile: $\log I \propto -r^{1/4}$ (here I is the intensity of light as a function of radius).[1]

We can also see a distinction between these two types of galaxies by looking at the distribution of all galaxies on a color-magnitude (CM) diagram. Absolute magnitude is logarithmically related to a galaxy's luminosity, the total amount of light emitted per second by an object. A larger magnitude indicates a dimmer object, while a lower magnitude indicates one that is brighter. The first CM diagram was introduced by Hertzsprung and Russell, when they plotted the spectral type of stars versus their magnitude. For individual stars, the spectral type is closely linked to the effective temperature, which in turn is closely related to color. Hence the Hertzsprung-Russell diagram is indeed a CM diagram. Still in use today, it suggests a positive relationship between temperature and luminosity for individual stars. While this relationship does not necessarily carry over for galaxies, the CM diagram still gives us an effective way to examine our two populations. The bottom panel of Figure 1 shows a CM diagram plotting our sample in the color index, *u*-*r*, versus *r*-band absolute magnitude. In *u*-*r*, one of many indexes used to measure color, a smaller value indicates a bluer object. The distribution is bimodal, with late type galaxies appearing bluer as compared to the redder early type galaxies. Absolute magnitudes are calculated from apparent magnitudes assuming a flat ΛCDM cosmology ($\Omega_{M,0}$ = 0.3089, $\Omega_{\Lambda,0}$ = 0.6911, H_0 = 67.74 km/sec/Mpc).[2] As a measure of comparison, our Milky Way has an absolute magnitude of $M_r = -21.83^{+0.38}_{-0.37}$.[3] Unfortunately, the color index of the Milky Way is not as well known.

The observed bimodality in CM space was first identified qualitatively in 1982 by Tully et al.[4] Strateva et al.[5] quantified the separation by providing a simple color cut at all luminosities to divide early type and late type galaxies. Baldry et al. 2004[6] later added luminosity dependence to this result by mathematically modeling both populations and finding an effective divider between them. By doing this, Baldry et al. presented a functional divider between the red and blue populations in CM space. This divider is shown as the cyan line overlaid on the CM diagrams of Figure 1.

The area in CM space immediately surrounding this divider, where the red and blue populations overlap, came to be known as the Green Valley (GV). This term was first used to describe the area separating the red and blue sequences in several 2007 papers studying the evolution of galaxy populations at high redshift[7]. It has been hypothesized that galaxies within this ill-defined

[1] Unterborn and Ryden (2008)
[2] Planck Collaboration XIII (2016)
[3] Licquia, Newman, and Brinchmann (2015b)
[4] Tully et al. (1982)
[5] Strateva et al. (2001)
[6] Baldry et al. (2004)
[7] Gerke et al. (2007); Cooper et al. (2007)

area are passively evolving after having their star formation mechanism turned off[8]. This makes sense – as stellar populations age and star formation continues, the gas necessary to form hot, blue stars is used up. The lack of these blue stars would cause the light emitted from the galaxy to become dominated by red giants, as opposed to a mix of blue and red giants. Throughout this process, a given galaxy could follow a track from the blue population toward the red population, passing through the GV. In addition, an excess of galaxies containing an Active Galactic Nucleus (AGN), a central black hole in a galaxy that is actively accreting matter, has been observed in the GV. This certainly provides motivation for further study.

In an effort to better probe the GV region of CM space, we provide a number of quantitative dividers between early type and late type populations on a CM diagram. These are based on the methods of Baldry et al. (2004), as well as the addition of morphological and spectroscopic information. We also analyze the distribution of galaxies containing an AGN in CM space, and we use our dividers to examine their presence in the GV region.

2. Data Acquisition:

To acquire our sample, we used data available through the twelfth data release (DR12) of the Sloan Digital Sky Survey (SDSS). The SDSS is a full-sky survey that through DR12 had imaged 14,555 square degrees of the celestial sphere.[9] Using a dedicated 2.5 meter telescope at Apache Point Observatory, the images were taken using five different filters (*ugriz*) as the telescope tracked great circles across the sky. These images are then passed through several pipelines which detect and measure the brightnesses, positions, and shapes of objects. The catalog of detected objects was then used to select targets for spectroscopic follow-up.[10]

The central wavelengths of the five Sloan *ugriz* filters are, in Angstroms, 3551, 4686, 6166, 7480, and 8932 respectively.[11] The throughput curves for each of the five Sloan filters are shown in Figure 2. This plot gives a measure of the amount of light detected by each filter as a function of wavelength. These throughput curves have evolved somewhat with time[12], but still give a good picture of the relative amount of light detected by each filter. The combination of these filters gives us good photometric data for any object across the full visible spectrum and into the near ultra-violet and near infrared. For our study, we use the *r*-band magnitude as a measure of luminosity because it covers a good portion of the visible spectrum where a lot of starlight is emitted, and it has the best filter response of the five photometric bands. As a diagnostic for color, we use *u*-*r*; most of the u-band light received is emitted by hot O and B stars, so this gives

[8] Schawinski et al. (2014)
[9] Albareti et al. (2016)
[10] Abazajian et al. (2009)
[11] Gunn, Jim, SDSS-III camera filter throughput curves
[12] Doi et al. (2010)

us a good measure of how blue the light profile of a given galaxy is. Using *u-r* color also gives us a good way to compare our results with those of Baldry et al., as they used the same measure.

Our sample uses galaxies from the SDSS Legacy Survey, which contained both an imaging survey as well as a flux limited ($r \leq 17.77$) spectroscopic survey. As a result, both photometric and spectroscopic data are provided for all galaxies in our sample. The imaging footprint of the Legacy survey covers 8,423 square degrees of sky, while the spectroscopic footprint is slightly smaller at 8032 square degrees.[13] We took only galaxies (as determined by the Sloan pipeline) with spectroscopic redshifts greater than 0.004 to eliminate contaminating foreground objects. At this redshift, the flux limit of the survey corresponds to an absolute r-band magnitude of $M_r = -13.47$. To reduce the effects of galactic evolution, we apply an upper redshift limit of 0.25, corresponding to a lookback time of about 3 Gyr. At a redshift of 0.25, the flux limit will only allow us to see galaxies with $M_r \leq -22.77$. Our final sample consisted of 675,833 galaxies. Given the depth of our sample, we had to correct for the effects of redshift in our photometric data. This was done through k-corrections using code provided by Blanton and Roweis (2007).[14] These k-corrections give more accurate apparent magnitudes for what the galaxy would look like at redshift $z = 0$.

3. Dividing the Red and Blue Sequences

To study the region of overlap between the red and blue sequences, it is necessary to adequately define and separate each of these populations. Baldry et al. (2004) (hereafter BO4) provided the most widely used luminosity dependent divider between the red and blue sequences. They used a sample from an early data release of the SDSS which contained 66,846 galaxies in the redshift range $0.004 < z < 0.080$. Using our larger, deeper sample, we follow the procedure of B04 to find new dividers. We first reproduce the methods of B04, giving us a separation based on color. We also generate dividers based on other criteria in which the two populations differ, namely morphology and spectral features.

3.1 – Color Divider

Our first goal was to create a separation based on color according to the methods of B04 using our larger sample. We first split the distribution of galaxies in CM space into 100 magnitude bins in the range $-24.0 < M_r < -18.0$. By comparison, B04 had 16 magnitude bins ranging from -15.5 to -23.5. Both the red and blue sequences were then modelled as Gaussian distributions with means and standard deviations shown in Figure 3. A division point was then found within each magnitude bin utilizing the concepts of completeness (C) and reliability (R) originating in

[13] Abazajian et al. (2009)
[14] Blanton and Roweis (2007)

Strateva et al. (2001) and used in B04. Completeness represents the percentage of galaxies identified as a specific color that are on the correct side of the divider, e.g. the number of galaxies redward of the divider over the number of red galaxies (according to the Gaussian model) in that magnitude bin. Reliability gives a measure of the contamination of each sample, and is defined as the number of galaxies on one side of the divider that are actually that color. For example, the reliability of the red population, R_r, is the number of red galaxies redward of the divider over the total number of galaxies redward of the divider. The optimal separating points (the yellow points in Figure 4) were found by maximizing the figure of merit from B04,

$$\tau = C_r R_r C_b R_b. \quad (1)$$

This gave us a series of points, which we fit using a least squares method weighted by the number of galaxies in each bin. A good fit to the separation points was found to be a quadratic,

$$(u - r) = -0.018(M_r + 21)^2 - 0.137(M_r + 21) + 2.20. \quad (2)$$

The divider is shown as the green line in Figure 4. This divider should be used with caution for high luminosity galaxies. In this high luminosity region, the two populations are not entirely distinct. Figure 5 shows the Gaussian models for a selected sample of magnitude bins. Notice that at high luminosities (the first few bins), not only are the populations indistinct, but also that the blue sequence extends significantly redward of the red sequence. Though our bimodal Gaussian model here provides a good mathematical fit, the result does not make physical sense. This is simply our fitting algorithm trying to model a non-Gaussian distribution. Hence, any division based on these population models in this region must be used with care. However, as we move toward lower luminosities, the bimodal Gaussian fit does a good job of modeling each population separately. At low luminosities, the red sequence becomes underpopulated, and as a result the red Gaussian is sometimes poorly modelled (these are the outlying means seen at low luminosities in Figure 3). However, the fit still generally models the distribution well, as can be seen in the final plot of Figure 5, our third lowest magnitude bin.

We also find that rather than optimizing the Baldry figure of merit, a simple division based on the intersection points of the red and blue sequence models provides a good divider under most circumstances. These points of intersection are shown by the red points in Figure 4, and lie quite close to the yellow points which were actually used in our fit. Further, since our fit is weighted by the number of galaxies in each magnitude bin (and most of the galaxies lie in the region where the points lie closest to one another), the least squares fit to the intersection points diverges from our divider by less than 0.1 mag at any magnitude bin.

3.2 – Morphological Divider

We next sought to divide the populations on the basis of morphology rather than color. The Sloan pipeline returns a fracDeV parameter for each galaxy in each photometric band (*ugriz*) which describes how well fit the galaxy is by a de Vaucouleurs light profile versus an exponential light profile. Each galaxy is fitted with a pair of models. The first has a de Vaucouleurs profile[15]:

$$I(R) = I_e \exp\left(-7.67\left[(R/R_e)^{-1/4} - 1\right]\right), \quad (3)$$

which is truncated at $7R_e$ to go smoothly to zero at $8R_e$. The other has an exponential profile:

$$I(R) = I_e \exp[-1.68(R/R_e - 1)], \quad (4)$$

truncated beyond $3R_e$ to go smoothly to zero at $4R_e$. The Sloan pipeline then takes the best fitting model of each type, and finds the best fitting linear combination of the two models to the galaxy profile. The fraction of the light contributed by the de Vaucouleurs profile is the fracDeV parameter[16]. Using the r-band fracDeV of each galaxy, we were able to isolate populations with well-defined morphologies. Galaxies with fracDeV < 0.1 were taken as our disk population. Similarly, those galaxies with fracDeV > 0.9 were taken to be our population of ellipsoidal galaxies.

Having identified two morphologically distinct populations, we apply an inclination correction following the methods of Unterborn & Ryden (2008)[17] to our population of disks to reduce the effects of extinction by dust. The inclination correction essentially tells us what a given galaxy's color and luminosity would be were it face on rather than inclined to our point of view. The inclination corrected magnitude and color for our disk population as a function of their short to long axis ratio, q, are given by:

$$M_r^f = M_r - 1.274(\log_{10} q)^2 \quad (5)$$

$$(u-r)^f = (u-r) + \left[0.454 - 0.255\left(M_r^f + 20.5\right)\right]\log_{10} q. \quad (6)$$

This puts our two populations on more equal footing (since elliptical galaxies have little to no dust, and hence no extinction effects), and has the effect of making our disk population as a whole bluer and brighter.

To find our morphological divider, we follow a similar procedure to that of the color divider in section 3.1. We again split the distribution into 100 magnitude bins (in the same range as above). However, since we now have two distinct populations, there is no need to fit a Gaussian model.

[15] de Vaucouleurs (1948)
[16] Unterborn and Ryden (2008)
[17] Unterborn and Ryden (2008)

The means and standard deviations of our two populations (inclination corrected, low fracDeV galaxies and high fracDeV galaxies) are shown in Figure 6. To find our divider, we again maximize the completeness and reliability of each population within each bin using the Baldry figure of merit, τ. Then using a least squares fitting method, weighted by the number of galaxies, we find a good fitting morphological separator to again be a quadratic,

$$(u-r) = -0.009(M_r+21)^2 + 0.037(M_r+21) + 2.12. \quad (7)$$

This separator is shown as the cyan/maroon line in Figure 7. As opposed to our color divider, which follows the sharply peaked red model population towards high luminosities, this morphological divider becomes bluer for brighter galaxies. This is a combination of the fact that we have a better separation at most luminosities between the two populations in the morphological case, and that the disk population is less populated at high luminosities. Our algorithm gives an inconsistent location for the divider at lower luminosities because of the large distribution in color of high fracDeV galaxies in this regime. The large standard deviations seen in Figure 6 at low luminosities are a reflection of there being a relatively constant number of high fracDeV galaxies across a wide range of colors in this regime (see the distribution of the high fracDeV population in Figure 7). However, because of the weighting of the points, this does not drastically affect the divider fit. Also, it can be seen in Figure 7 that the morphological divider seems to hug the second contour of both the disk and tri-axial populations. This suggests (as we found for the color divider) that a division where there are equal numbers of each population would be just as effective in most cases as the figure of merit method. The divider should again be used with caution at very high luminosities ($M_r \lesssim -23$) where there are not enough disk galaxies to generate a reliable divider, and similarly at low luminosities ($M_r \gtrsim -18.7$) where the high fracDeV subsample is underpopulated.

3.3 – Spectroscopic Divider

Lastly, we separated our distribution of galaxies on the basis of their spectral features. The SDSS database has the results of two spectroscopic studies done on their LEGACY sample: one performed in collaboration between the Max Planck Institute for Astrophysics and Johns Hopkins University (MPA-JHU)[18], and the other performed by the Portsmouth group[19]. In each of these studies, galaxies are labelled according to their position in the BPT (Baldwin, Philips and Terlevich) diagram, which classifies galaxies according to the relative strengths of their emission lines, specifically the forbidden lines NII 6583Å and OIII 5007Å, as well as Hα and Hβ[20]. The lines NII and OIII come from photons emitted by electron transitions in ionized nitrogen and doubly ionized oxygen, respectively. Hα and Hβ correspond to the two lowest

[18] Brinchmann et al. (2004); Kauffmann et al. (2003a); Tremonti et al. (2004)
[19] Thomas et al. (2013); Maraston and Strömbäck (2011)
[20] Baldwin, Philips and Terlevich (1981)

energy transitions of the Hydrogen Balmer series, and occur at 6563Å and 4861Å, respectively. Figure 8 shows the galaxies in our sample with high amplitude over noise plotted on such a diagram. Late type galaxies generally have ongoing star formation, so we identify as our blueward population in this case galaxies classified as 'Star Forming.' Early type galaxies on the other hand are quiescent, so our redward population consists of galaxies with weak emission lines as compared to continuum level emissions.

We take as our primary spectroscopic study that done by the Portsmouth group because they provide amplitude over noise ratios for each of the lines used in BPT classification, allowing us to set the threshold below which we consider a galaxy (relatively) quiescent. A lower amplitude over noise limit of 1.0 for all four of the lines was imposed on our blue, star forming population, isolating those galaxies which are assuredly undergoing star formation. Any galaxy with amplitude over noise less than 1.0 for two or more of the four lines was included in our red population, as well as those galaxies classified as 'BLANK' in the Portsmouth study (indicating their emission lines were so weak as to be unrecognizable, or the emission line data was unavailable). Galaxies with only one emission line having amplitude over noise less than one were ambiguous, so they were discarded from the sample.

The means and standard deviations of our two populations in each magnitude bin are shown in Figure 9. Equipped with our two populations, we follow the same procedure as in our morphological divider – splitting the distribution into 100 magnitude bins and optimizing the Baldry figure of merit within each bin. Fitting to these points again with weighted least squares methods, we find a good fitting separator to again be a quadratic,

$$(u - r) = -0.047(M_r + 21)^2 - 0.016(M_r + 21) + 2.28. \quad (8)$$

The spectroscopic separator is plotted as the solid cyan/maroon line in Figure 10. As with the morphological separator, the blue population is underpopulated at high luminosities ($M_r \lesssim -23$), so the separator should be used cautiously in this regime. For the purpose of comparison, we repeat this same process for the MPA-JHU study. Without signal to noise data provided, we take as our blue population galaxies identified as 'Star Forming' and as our red population those labeled as 'Unclassifiable,' meaning they have no or very weak emission lines. The separator achieved from this study is shown in Figure 10 as the dashed black line. This separator is very comparable to the divider using data from the Portsmouth study, except at higher luminosities. In this region, the MPA-JHU divider extends redward of the Portsmouth divider, mainly because the star forming population as defined by MPA-JHU extends further redward than does that of the Portsmouth study. The majority of these red star forming galaxies are removed from our blueward population when we impose the amplitude over noise cut.

4. Galaxies with AGN in the Green Valley

After finding effective separators for the red and blue populations in CM space, we sought to analyze the galaxy populations present in the GV region. We accomplished this primarily using spectroscopic information on our galaxies. Both the MPA-JHU and Portsmouth studies provide classifications for galaxies based on their emission line characteristics according to the BPT diagram. Figure 8 shows how a galaxy is classified based on its location on the BPT diagram. Star forming galaxies are galaxies whose emission characteristics suggest there has been recent star formation. Composite galaxies have emission characteristics suggestive of both star formation and an Active Galactic Nucleus. Galaxies with AGN are divided into two types: Seyferts and galaxies with Low-Ionization Nuclear Emission-line Regions (LINERs). Seyfert galaxies are the first ever identified type of galaxy with an AGN, and are characterized by relatively low luminosity central regions (as compared to quasars, which are very bright). LINERS have a very low nuclear luminosity. They closely resemble Seyfert galaxies spectroscopically, except that their low ionization lines (like OI 6548Å and NII 6583Å) are stronger. The division between Seyferts and LINERS is found by empirically separating the two populations in BPT space once they have been identified by other emission line ratios.[21] The dividing line between composite galaxies and AGN galaxies is a theoretical upper limit on the location of star forming galaxies on the BPT diagram.[22] The line separating composites from star forming galaxies comes from an analysis by Kauffmann et al.[23] which finds a lower limit for the location of AGN galaxies in BPT space.

Our studies primarily focused on the galaxies containing an AGN. As aforementioned, astronomers have observed an excess of galaxies with an AGN in the GV region. The spectroscopic study done by the Portsmouth group classified galaxies with AGN as either Seyferts or LINERs according to the division of Schawinski et al. (2007). The MPA-JHU study simply classified all of them as AGN galaxies. Figure 11 shows the distribution of these AGN galaxies relative to our three dividers. Seyfert galaxies generally fall slightly blueward of LINERs, and the two studies appear to be consistent, as the MPA-JHU "AGN" galaxies appear to be approximately a combination of the two Portsmouth distributions. Figure 12 shows the means and standard deviations of these three populations (Seyferts, LINERs, and MPA AGN). We see similarly here that the Seyferts lie blueward of the LINERs, and are in general more widely distributed in color (though there are also significantly less of them).

We can also look at the fraction of each bin that is classified as a Seyfert, LINER, or AGN galaxy. This is what is shown in Figure 13. We do indeed see an overdensity of AGN galaxies as classified by MPA-JHU in the GV region. In fact, this "AGN ridge" aligns very well with the ill-defined GV region spanned by our three dividers. We see a similar pattern in Seyferts from the

[21] Schawinski et al (2007)
[22] Kewley et al. (2001)
[23] Kauffmann et al. (2003c)

Portsmouth data in this same region. However, LINERs are much more broadly distributed across CM space. It appears as though our spectroscopic divider very roughly delineates a region of sharp increase in the fraction of LINER galaxies. This could indicate that LINERs are more likely to be quiescent galaxies than to be actively forming stars. High fractions of AGN galaxies of all types are also present along the fringes of our distribution in Figure 13. This could be motivation for further study of these 'abnormal' galaxies. Figure 14 shows the fraction of galaxies identified to contain an AGN by the Portsmouth group (both Seyferts and LINERS) that are classified as Seyferts. This further confirms the location of Seyferts in the GV, but also shows that the transition from high Seyfert fraction to high LINER fraction is somewhat gradual through the GV. This transition occurs blueward of the steep increase in LINER fraction seen in Figure 13. The location of Seyferts and LINERs in CM space could give us clues as to why a Low-Ionization Nuclear Emission-line Region might appear in a given galaxy.

Having confirmed an AGN overdensity in the GV region, we then wanted to see where galaxies in the GV (as defined by our dividers) fell on the BPT diagram. Figure 15 shows the BPT distribution of high amplitude over noise galaxies within 0.05 mag in u-r color of our three different dividers. It does not appear that there is any significant propensity toward a particular region of the BPT diagram for galaxies in the GV. However, in both the color divider and spectroscopic divider case, there is a star forming 'arc' that travels along the Kauffmann (star forming/composite) divider. This arc is heavily populated in Figure 8. However, few galaxies surrounding our morphological divider fall along this arc. This suggests that this star forming arc is populated by galaxies in a region of CM space that the morphological divider does not traverse.

5. Discussion and Conclusion

By performing methods identical to that of B04, we are able to examine the effects of a larger, deeper sample on a division between galaxy populations. We find that our divider continues to extend redward for increasing luminosities, whereas the divider of B04 stayed relatively constant in this region. We also find that the optimal separation between our early type and late type populations is dependent on the information used to distinguish between them. Because of this, it does not appear possible to assign an overall shape or slope to the Green Valley as a whole; even with the results of this analysis, it is still a poorly defined region. Nonetheless, the quantitative dividers provided here could be quite useful in the field. Large data studies are becoming increasingly prevalent in the field of astronomy. It is hoped that our morphological and spectroscopic dividers, as well as the improved color divider, can provide a reliable way to isolate populations for independent study.

There is certainly room for further analysis of the presence of galaxies with an AGN in the GV region. It has been theorized that active galactic nuclei play a role in galactic evolution, whether

it be through the quenching of star formation or some other mechanism. The peculiarities noted in this study, in particular the agreement of certain dividers with the observed "AGN ridge," could provide some insight into the evolutionary processes of galaxies moving through the GV region. Moreover, the characteristics of galaxies surrounding our dividers point to the potential existence of spectroscopically unique populations within CM space.

References:

Abazajian, K. N. et al. (2009), The Astrophysical Journal Supplement, vol. 182. pp. 543-558, June 2009.

Albareti et al. (2016), preprint; arXiv: 1608.02013.

Baldry, I. K. et al. (2004), The Astrophysical Journal, vol. 600. pp. 681-694, January 2004.

Baldwin, J. A., Philips, M. and Terlevich, R. (1981), Publications of the Astronomical Society of the Pacific, vol. 93. pp. 5-19, February 1981.

Blanton, M. R. and Roweis, S. (2007), The Astronomical Journal, vol. 133. pp. 734-754, February 2007.

Brinchmann, J. et al. (2004), Monthly Notices of the Royal Astronomical Society, vol. 351. pp. 1151-1179, July 2004.

Cooper, M. C. et al. (2007), Monthly Notices of the Royal Astronomical Society, vol. 376. pp. 1445-1459, April 2007.

de Vaucouleurs, G. (1948), Annales d'Astrophysique, vol. 11. p.247, January 1948.

Doi, M. et al. (2010), The Astronomical Journal, vol. 139. pp. 1628-1648, April 2010.

Gerke, B. F. et al. (2007), Monthly Notices of the Royal Astronomical Society, vol. 376. pp. 1425-1444, April 2007.

Gunn, Jim, SDSS-III Camera Filter Throughput Curves. http://www.sdss.org/instruments/camera/#Filters.

Maraston, C. and Strömbäck, G. (2011), Monthly Notices of the Royal Astronomical Society, vol. 418. pp. 2785-2811, December 2011.

Kauffmann, G. et al. (2003a), Monthly Notices of the Royal Astronomical Society, vol. 341. pp. 33-53, May 2003.

Kauffmann, G. et al. (2003c), Monthly Notices of the Royal Astronomical Society, vol. 346. pp. 1055-1077, December 2003.

Kewley, L. J. et al. (2001), The Astrophysical Journal, vol. 556. pp. 121-140, July 2001.

Licquia, T. C., Newman, J. A. and Brinchmann, J. (2015b), The Astrophysical Journal, vol. 809. Article id. 96, 19 pp., August 2015.

Planck Collaboration XIII (2016), Astronomy & Astrophysics 594, id. A13, 63 pp., September 2016.

Schawinski, K. et al (2007), Monthly Notices of the Royal Astronomical Society, vol. 382. pp. 1415-1431, December 2007.

Schawinski, K. et al. (2014), Monthly Notices of the Royal Astronomical Society, vol. 440. pp. 889-907, May 2014.

Strateva, I. et al. (2001), The Astronomical Journal, vol. 122. pp. 1861-1874, October 2001.

Thomas, D. et al. (2013), Monthly Notices of the Royal Astronomical Society, vol. 431. pp. 1383-1397, May 2013.

Tremonti, C. A. et al. (2004), The Astrophysical Journal, vol. 613. pp. 898-913, October 2004.

Tully, R. B., Mould, J. R. and Aaronson, M. (1982), The Astrophysical Journal, vol. 257. pp. 527-537, June 1982.

Unterborn, C. T. and Ryden, B. S. (2008), The Astrophysical Journal, vol. 687. pp. 976-985, November 2008.

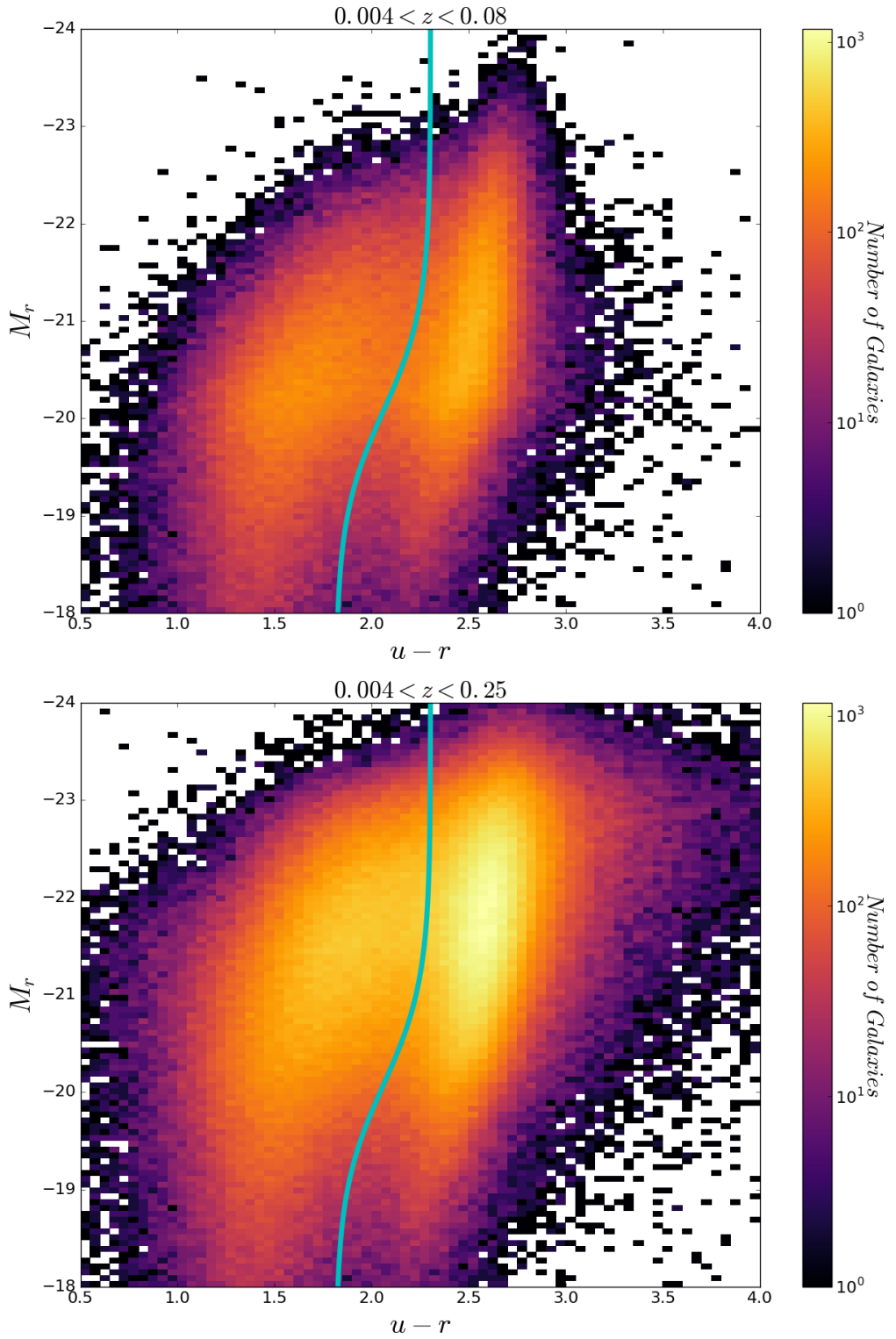

Figure 1: CM diagram with a redshift cut at z = 0.08 (top panel) and z = 0.25 (bottom panel). The top panel shows 212,008 galaxies as opposed to B04's 66,846 because it is simply a redshift-limited subsample of our original sample in the bottom panel. Notice that by increasing our depth, we primarily add high luminosity galaxies to our sample.

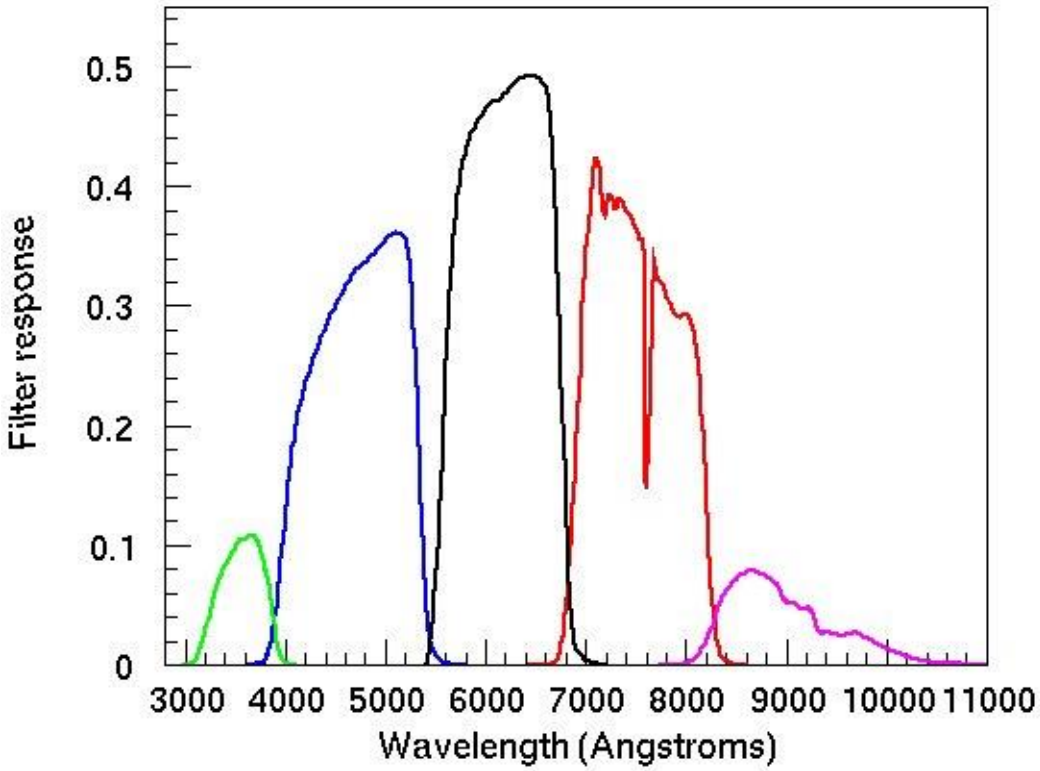

Figure 2: Shown here are the throughput curves for the five Sloan *ugriz* filters. In the figure, *u* is the green curve, *g* is blue, *r* is black, *i* is red, *z* is pink. The high response of the *r* filter is a large reason why we use it for our absolute magnitudes. (Image Credit: Jim Gunn, SDSS)[24]

[24] Gunn, Jim, SDSS-III camera filter throughput curves

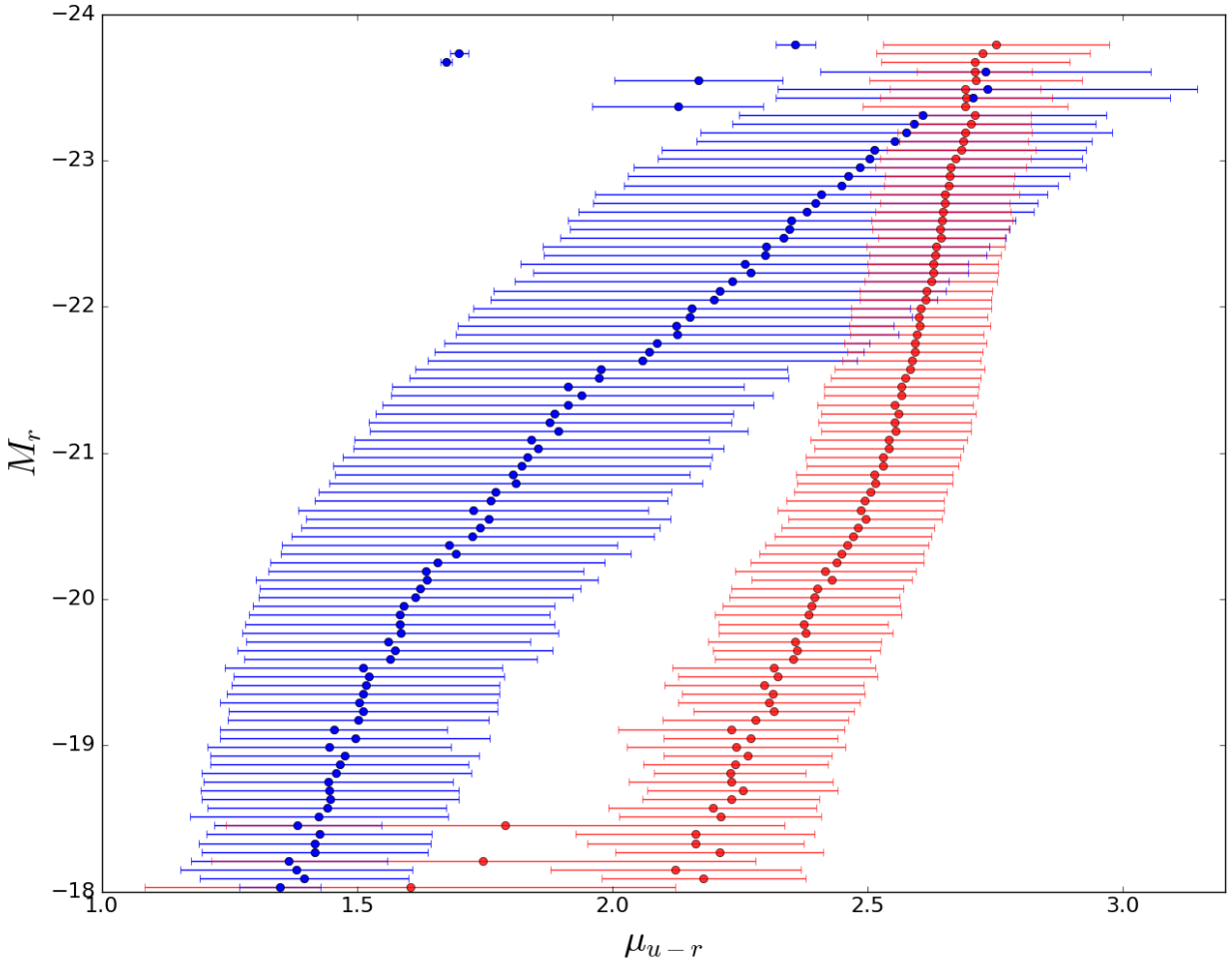

Figure 3: Means (points) and standard deviations (error bars) of the blue and red model populations as a function of magnitude. The red sequence stays relatively narrow while becoming slightly redder toward higher luminosities. The blue population curves even further redward and becomes much wider to account for the non-Gaussian distribution in this regime.

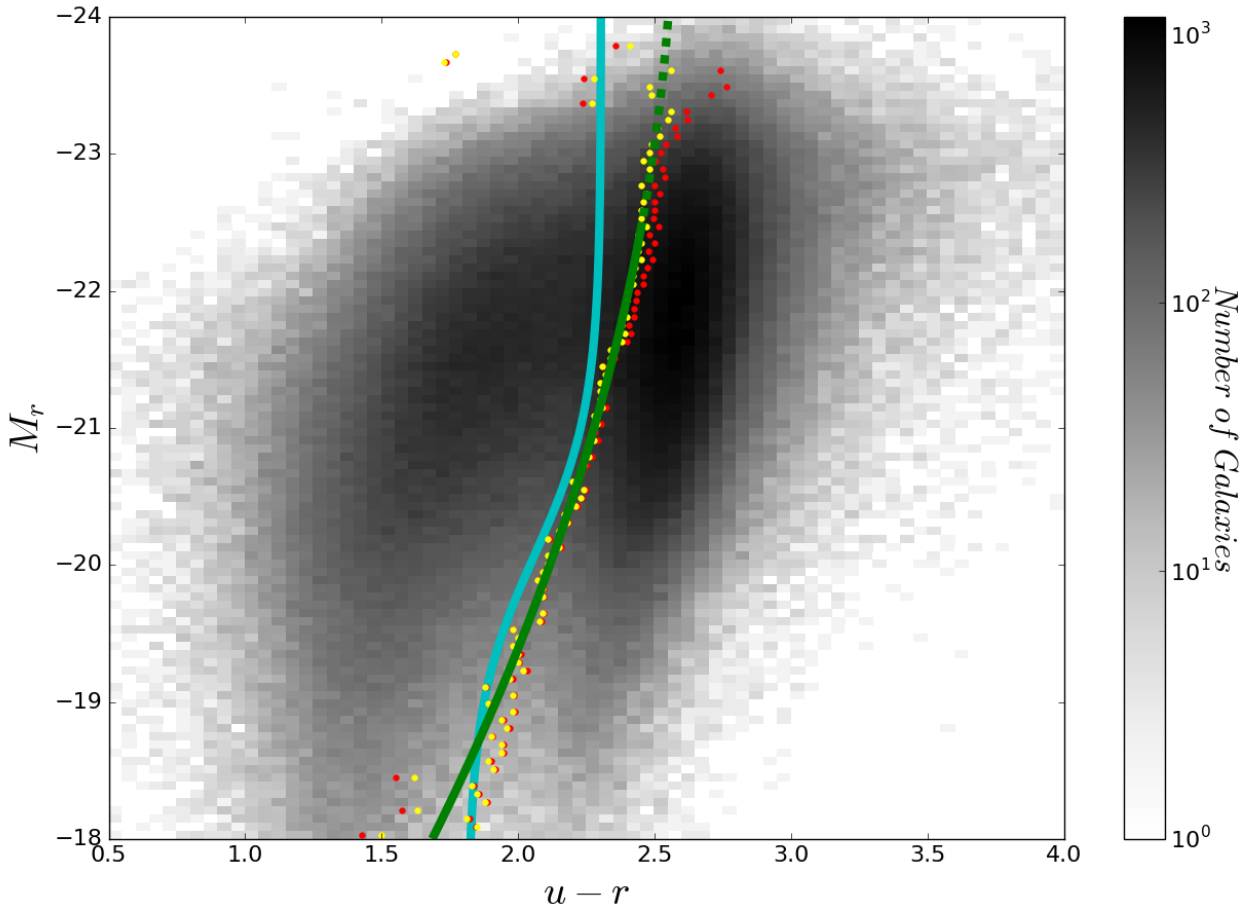

Figure 4: The color divider given in green, with the B04 divider plotted in cyan. Yellow points are the positions at which our figure of merit is optimized for a given magnitude bin. Red points are the intersections of the two populations. The dashed portion of the green line denotes the region where the red and blue sequences converge, causing our algorithm to model unphysical populations.

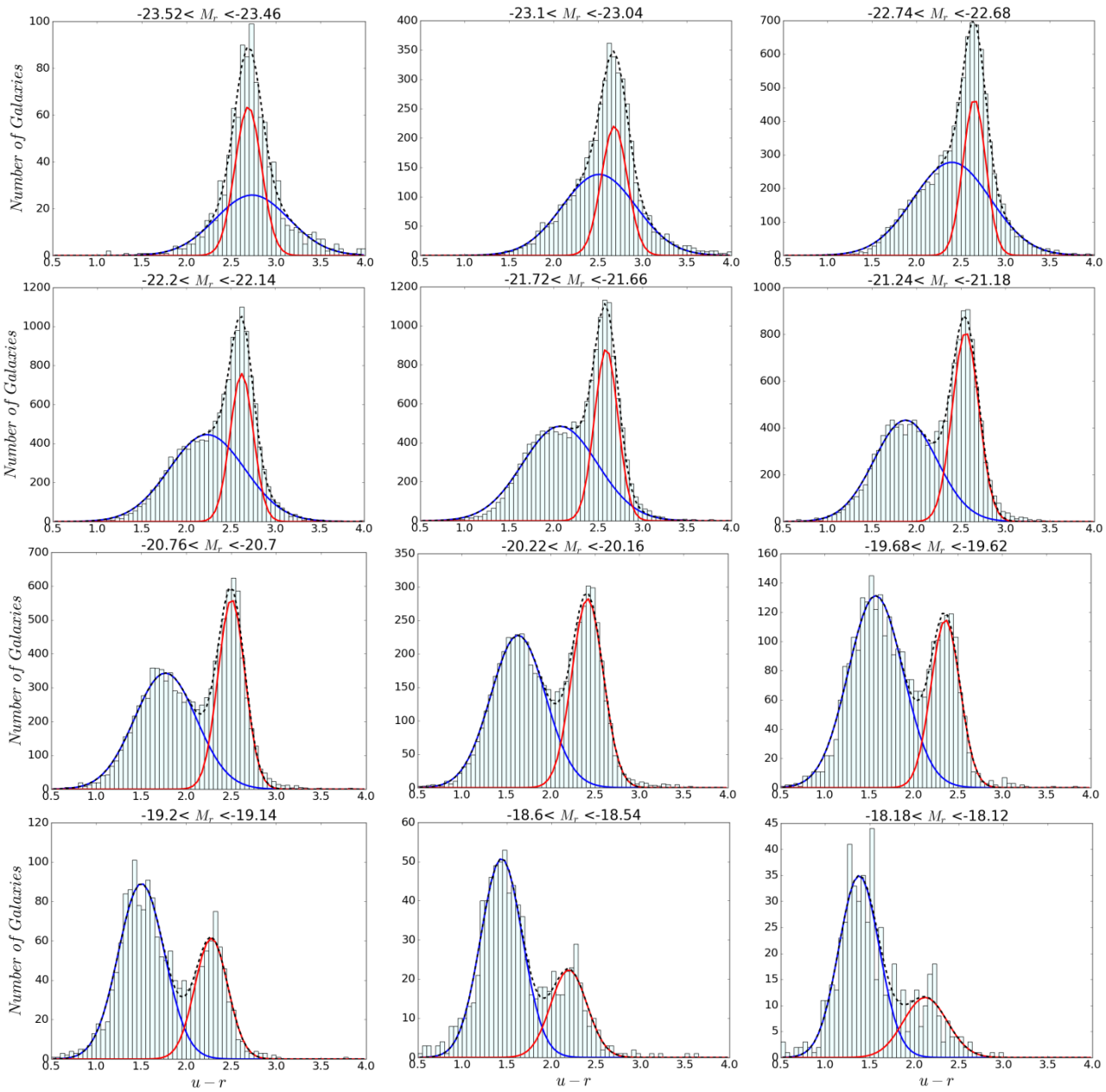

Figure 5: Model populations overlaid on the actual distribution for a selected sample of magnitude bins. At high luminosities, the distribution is not Gaussian, so our fitting algorithm models a wide blue population to account for the wide tails. However, as we move toward lower luminosities, the models more effectively separate the two populations.

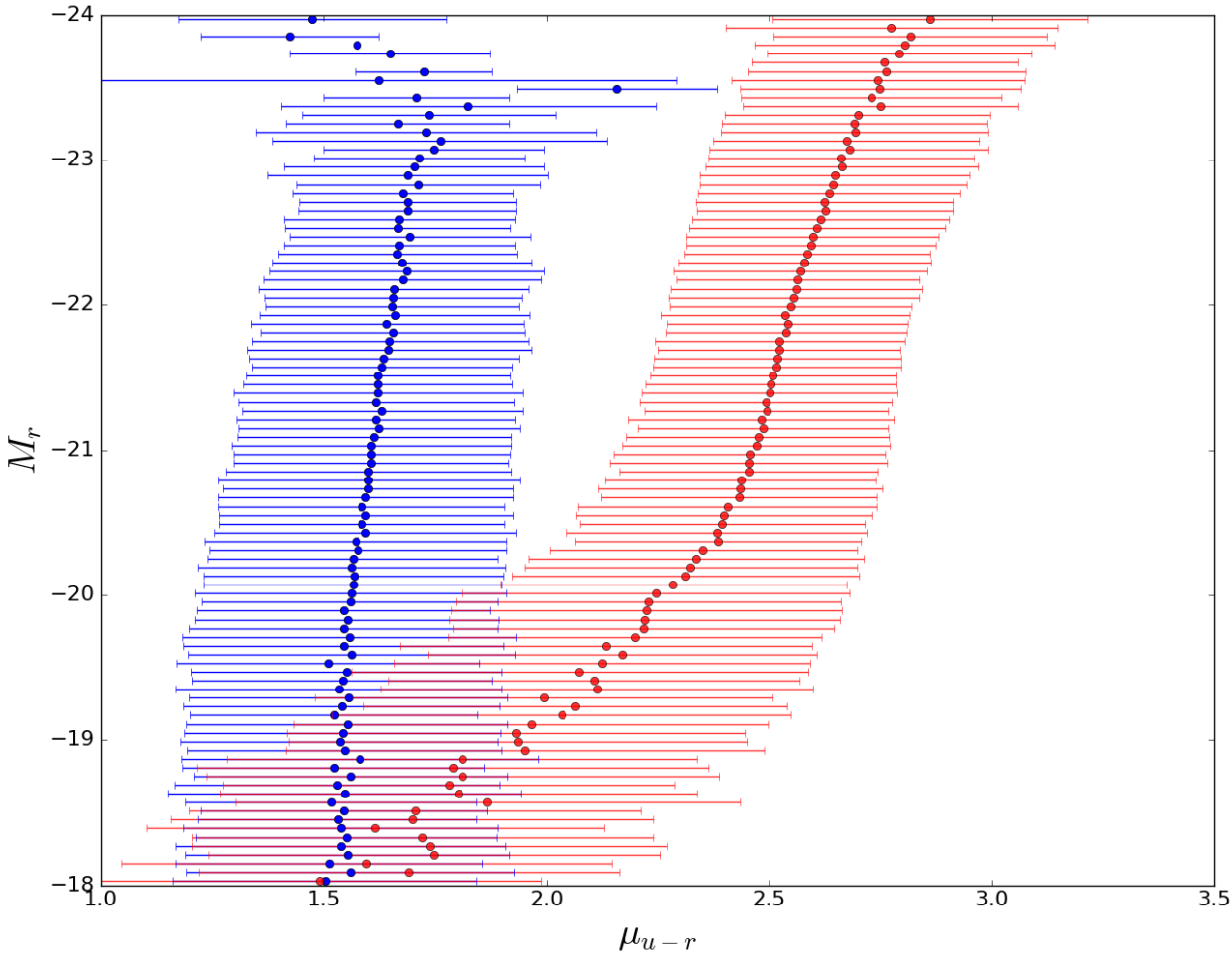

Figure 6: Means (points) and standard deviations (error bars) of the inclination corrected disk population (blue) and the high fracDeV, ellipsoidal population (red). Disk galaxies are very scarce at high luminosities ($M_r \lesssim -23.5$), so the means are very sporadic. The widening and blueward movement of the red population at low luminosities reflect the wide distribution in color of high fracDeV galaxies in this regime (see lower luminosity red distribution in Figure 7).

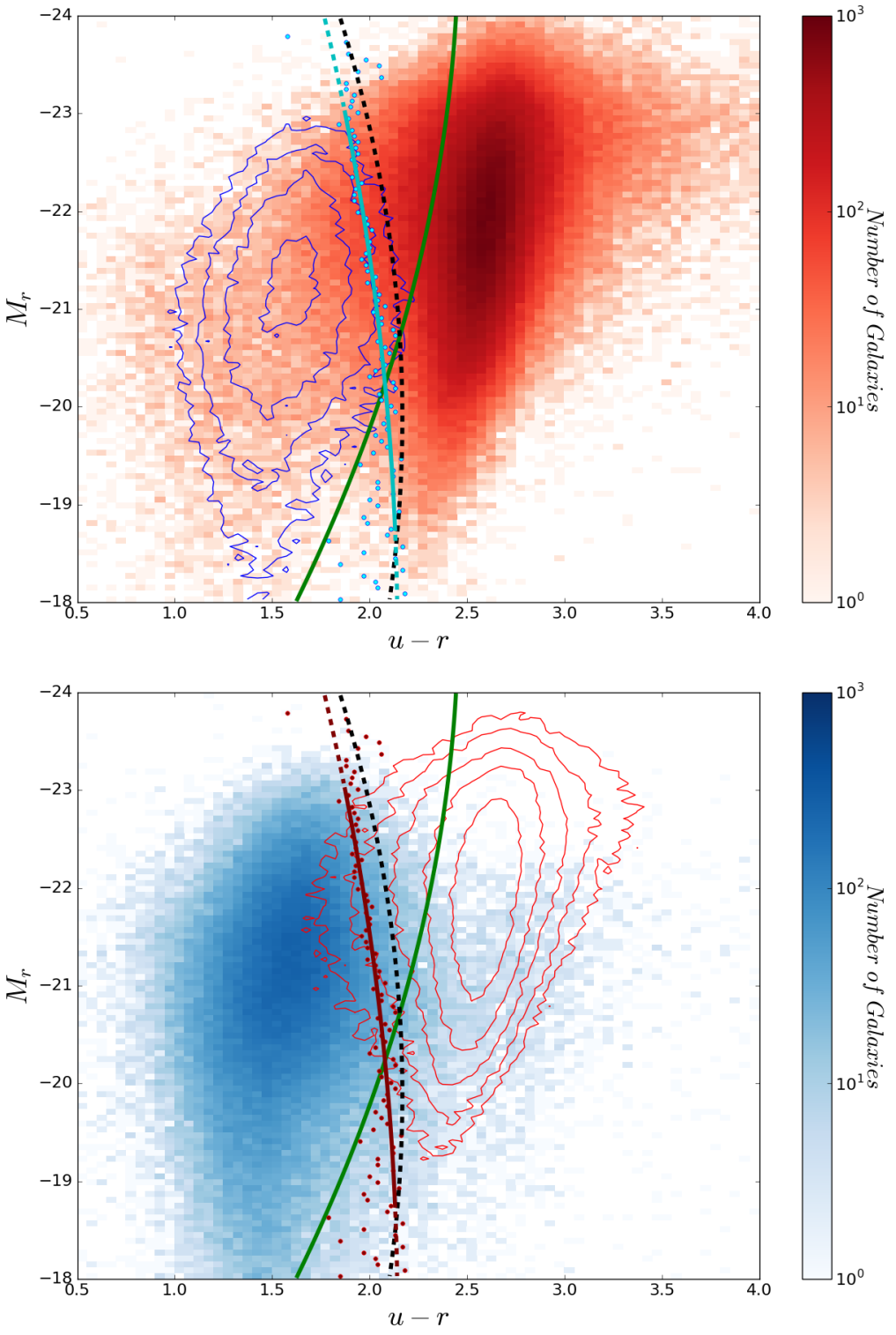

Figure 7: Morphological divider in cyan/maroon, with our color divider shown in green for reference. The points where our tau parameter is optimized are shown, as well as the disk (blue) and ellipsoidal (red) populations in both contour and histogram form. The dashed black line shows the location of the divider for a non-inclination corrected disk population (distribution not shown). The contours are spaced by $10^{n/3}$, with the lowest contour corresponding to $n = 4$.

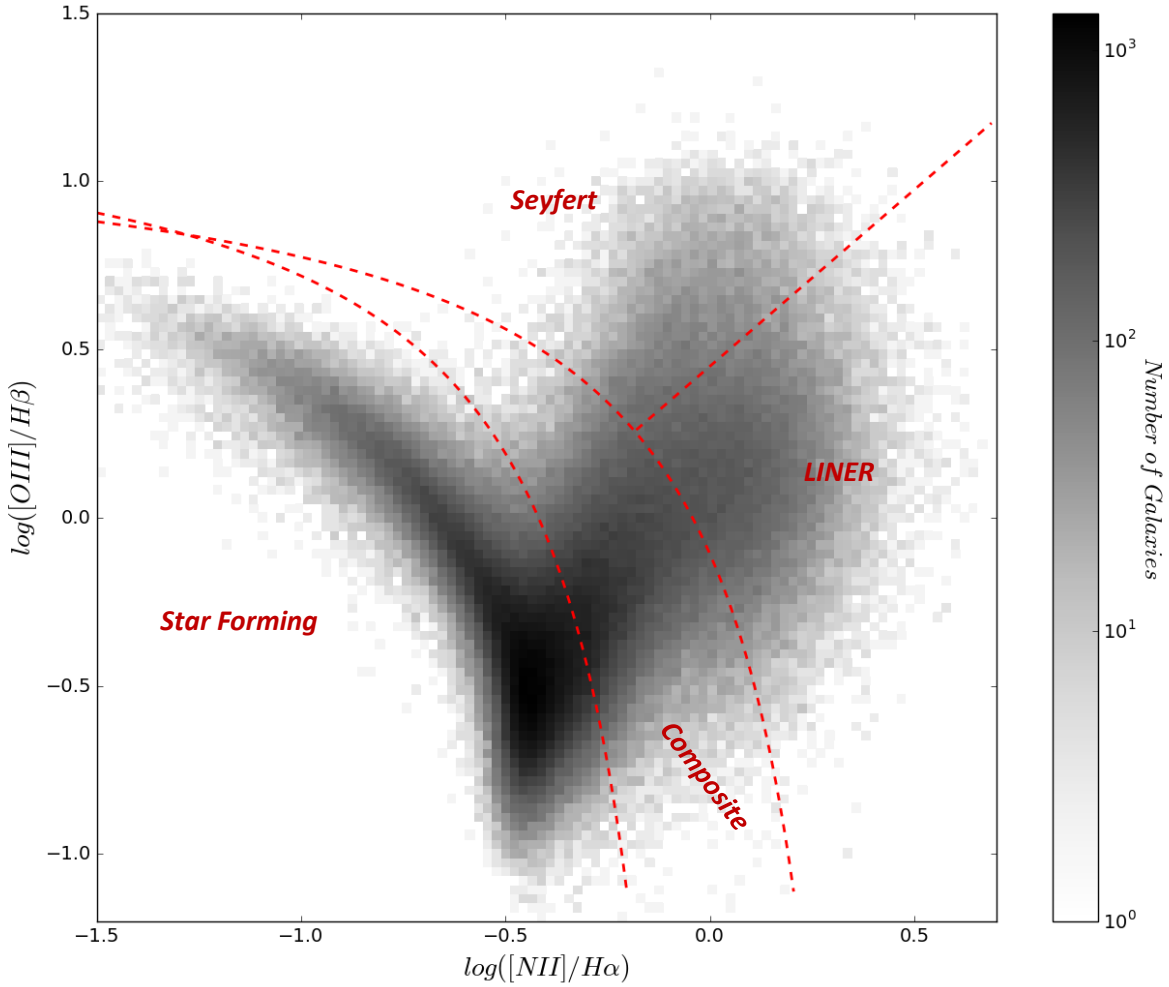

Figure 8: A BPT diagram of high amplitude over noise galaxies in our sample. The axes are the logarithmically scaled ratios of the flux of each emission line denoted (*NII/Hα, OIII/*Hβ). Overlaid are the dividing lines between star forming, composite, Seyfert and LINER galaxies.[25]

[25] Schawinski et al (2007); Kewley et al. (2001); Kauffmann et al. (2003c)

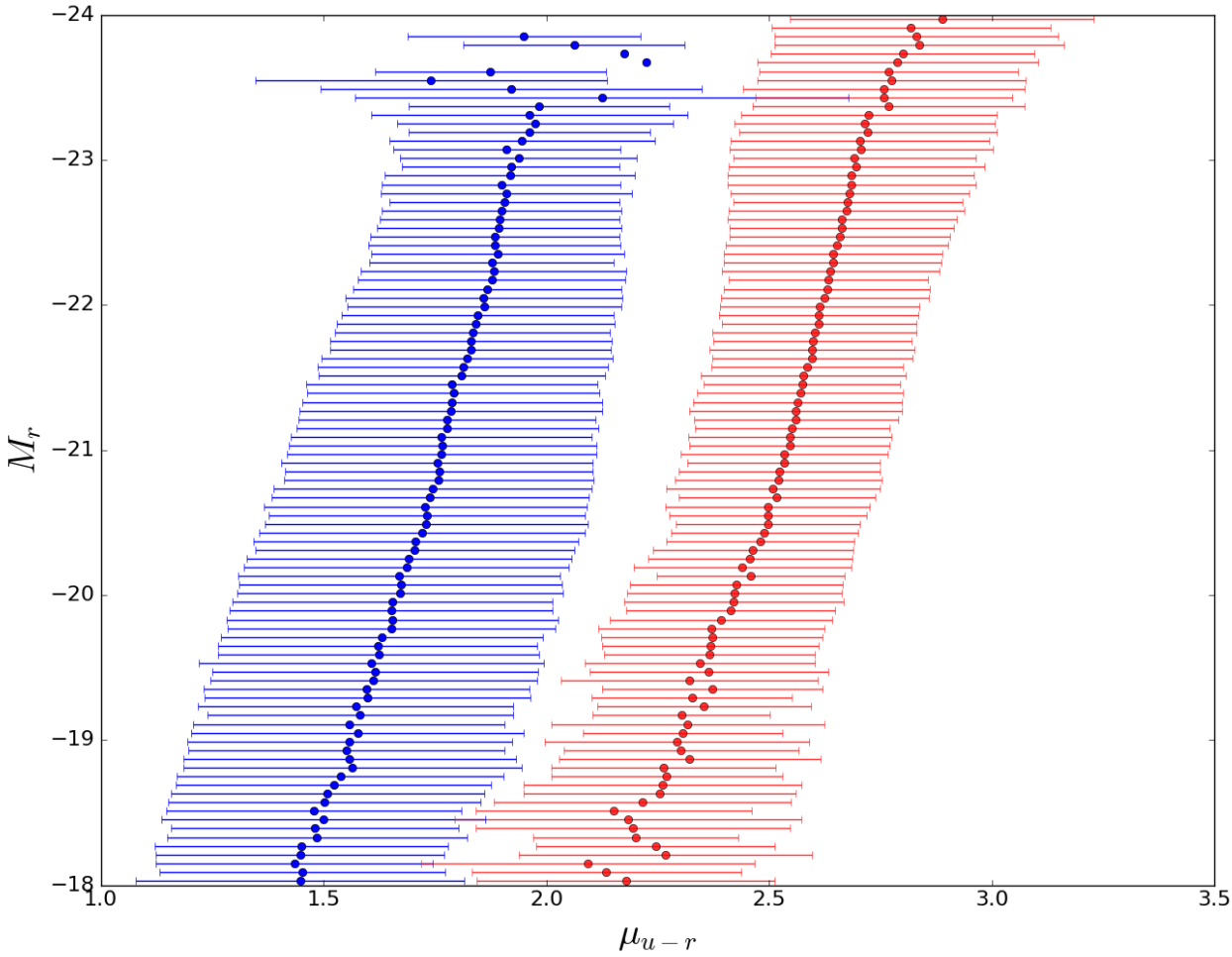

Figure 9: Means (points) and standard deviations (error bars) for the star forming (blue) and low amplitude over noise (red) galaxies used in our spectroscopic division. The populations are not as well separated as the means make them appear. At high luminosities, our star forming population is underpopulated leading to the sporadic means and standard deviations in this regime.

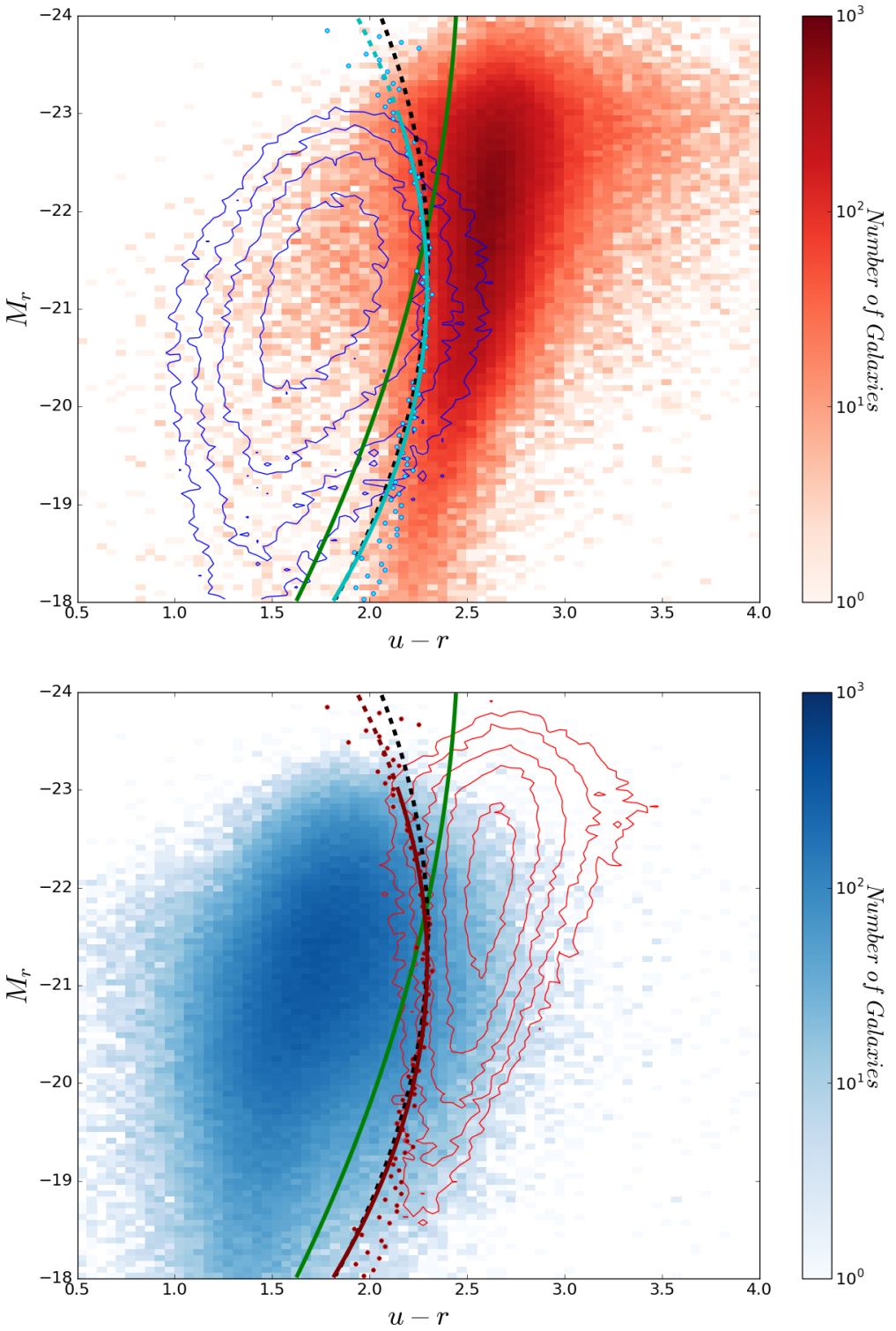

Figure 10: Our spectroscopic divider plotted in cyan/maroon, with our color divider overlaid in green. The points where our tau parameter is optimized are shown, as well as both the star forming (blue) and low amplitude over noise (red) populations in both contour and histogram form. The dashed black line is the divider using the MPA study (populations not shown here). Contours are spaced according to $10^{n/3}$, with the lowest contour at $n = 4$.

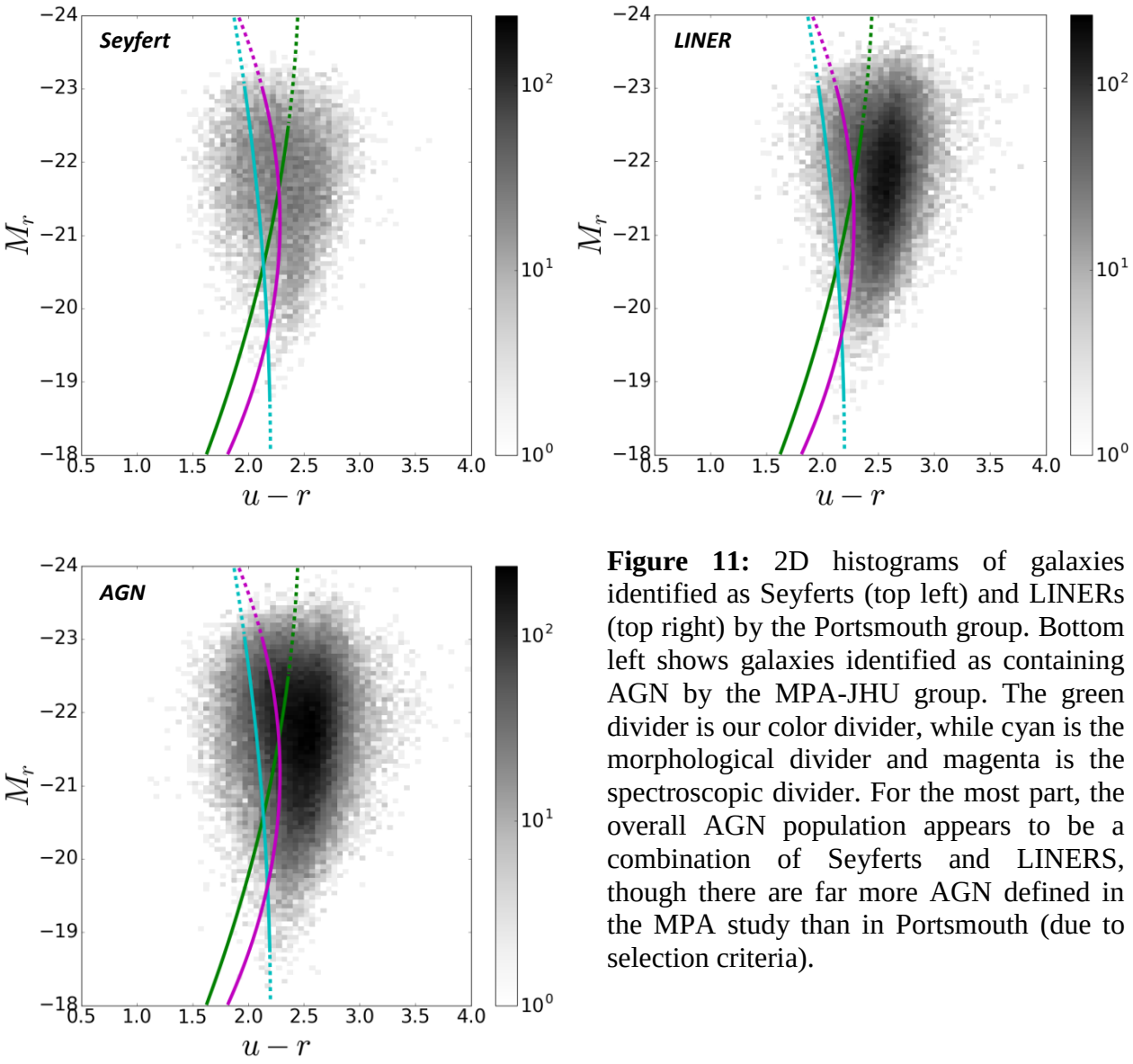

Figure 11: 2D histograms of galaxies identified as Seyferts (top left) and LINERs (top right) by the Portsmouth group. Bottom left shows galaxies identified as containing AGN by the MPA-JHU group. The green divider is our color divider, while cyan is the morphological divider and magenta is the spectroscopic divider. For the most part, the overall AGN population appears to be a combination of Seyferts and LINERS, though there are far more AGN defined in the MPA study than in Portsmouth (due to selection criteria).

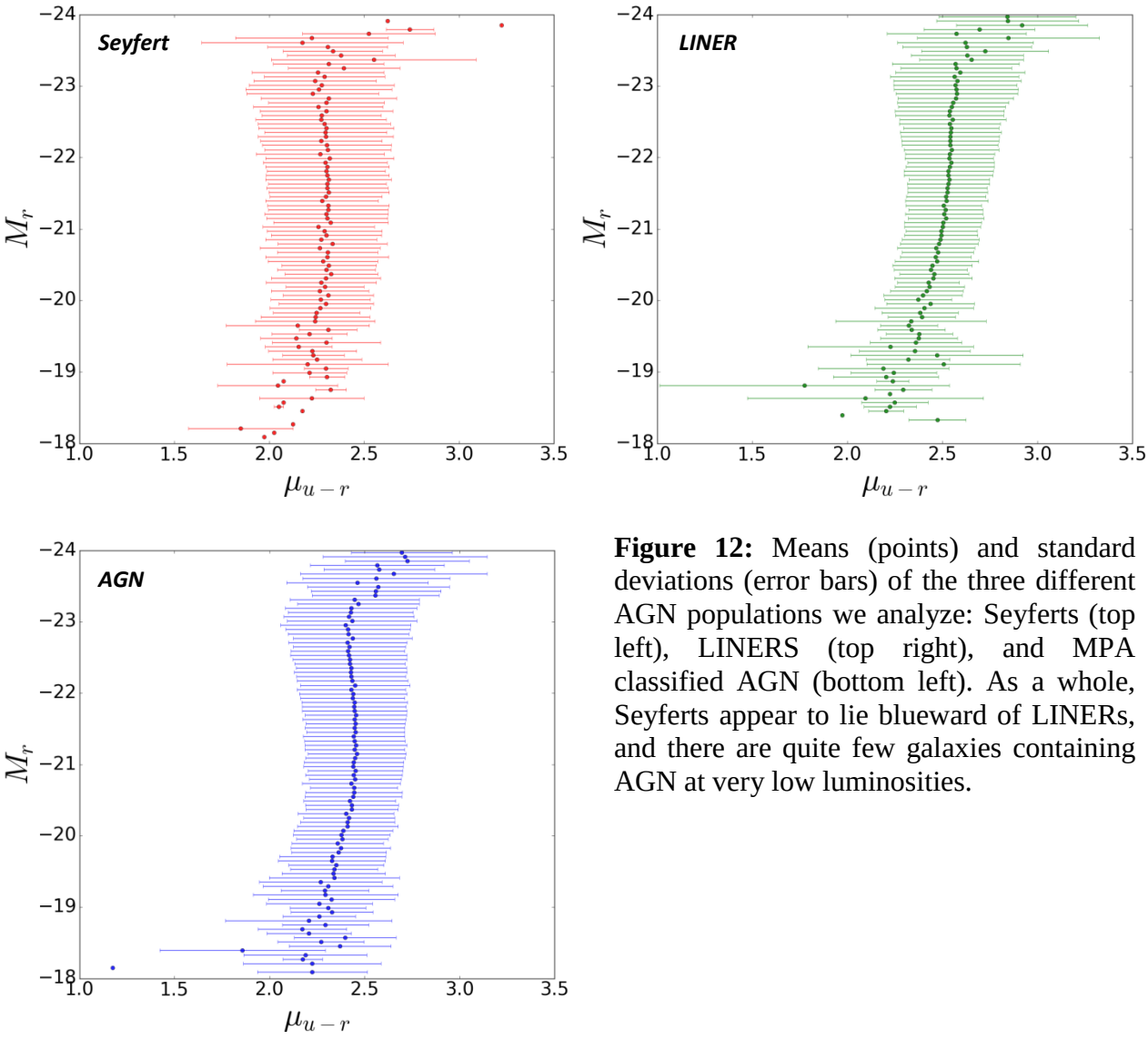

Figure 12: Means (points) and standard deviations (error bars) of the three different AGN populations we analyze: Seyferts (top left), LINERS (top right), and MPA classified AGN (bottom left). As a whole, Seyferts appear to lie blueward of LINERs, and there are quite few galaxies containing AGN at very low luminosities.

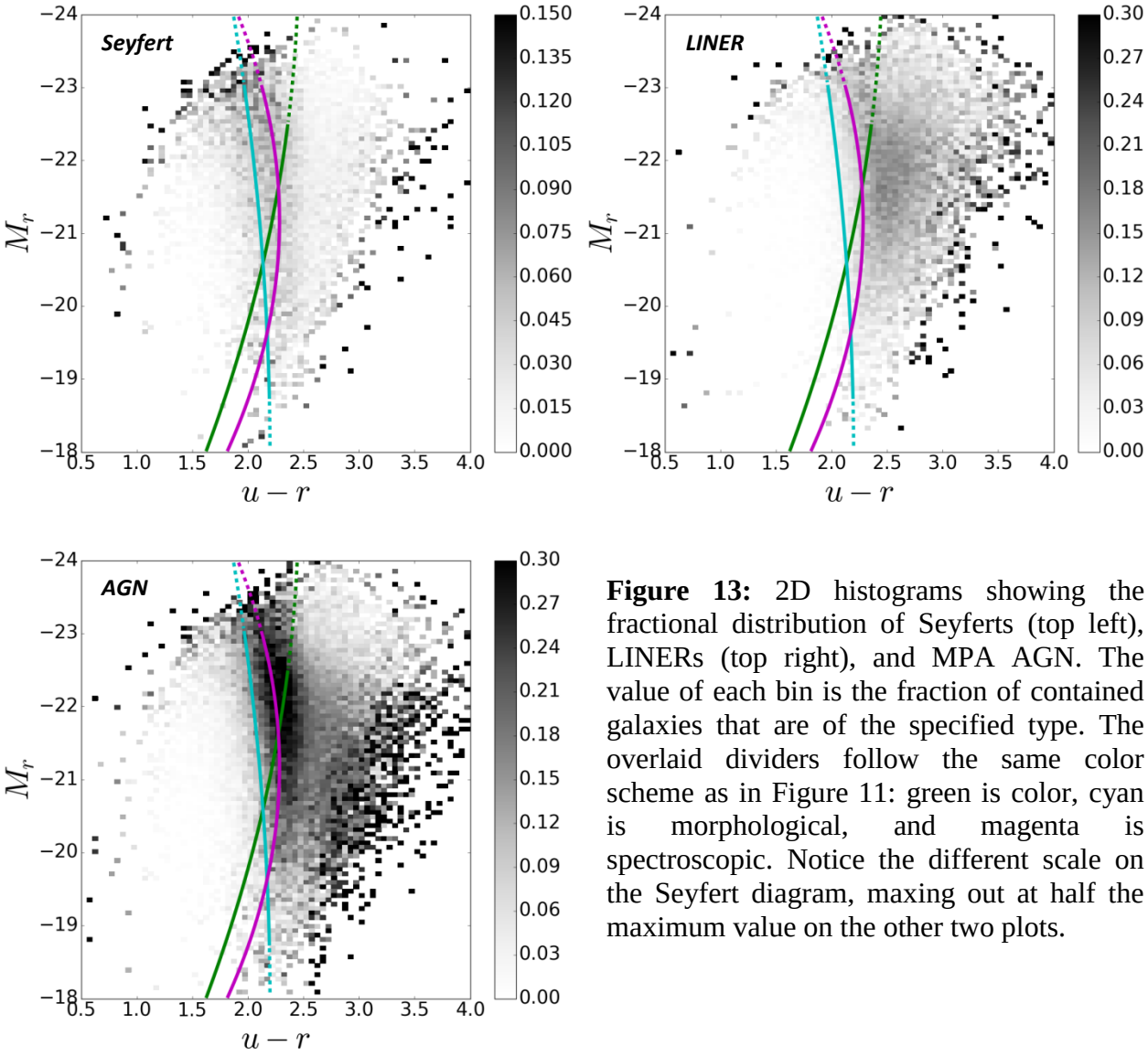

Figure 13: 2D histograms showing the fractional distribution of Seyferts (top left), LINERs (top right), and MPA AGN. The value of each bin is the fraction of contained galaxies that are of the specified type. The overlaid dividers follow the same color scheme as in Figure 11: green is color, cyan is morphological, and magenta is spectroscopic. Notice the different scale on the Seyfert diagram, maxing out at half the maximum value on the other two plots.

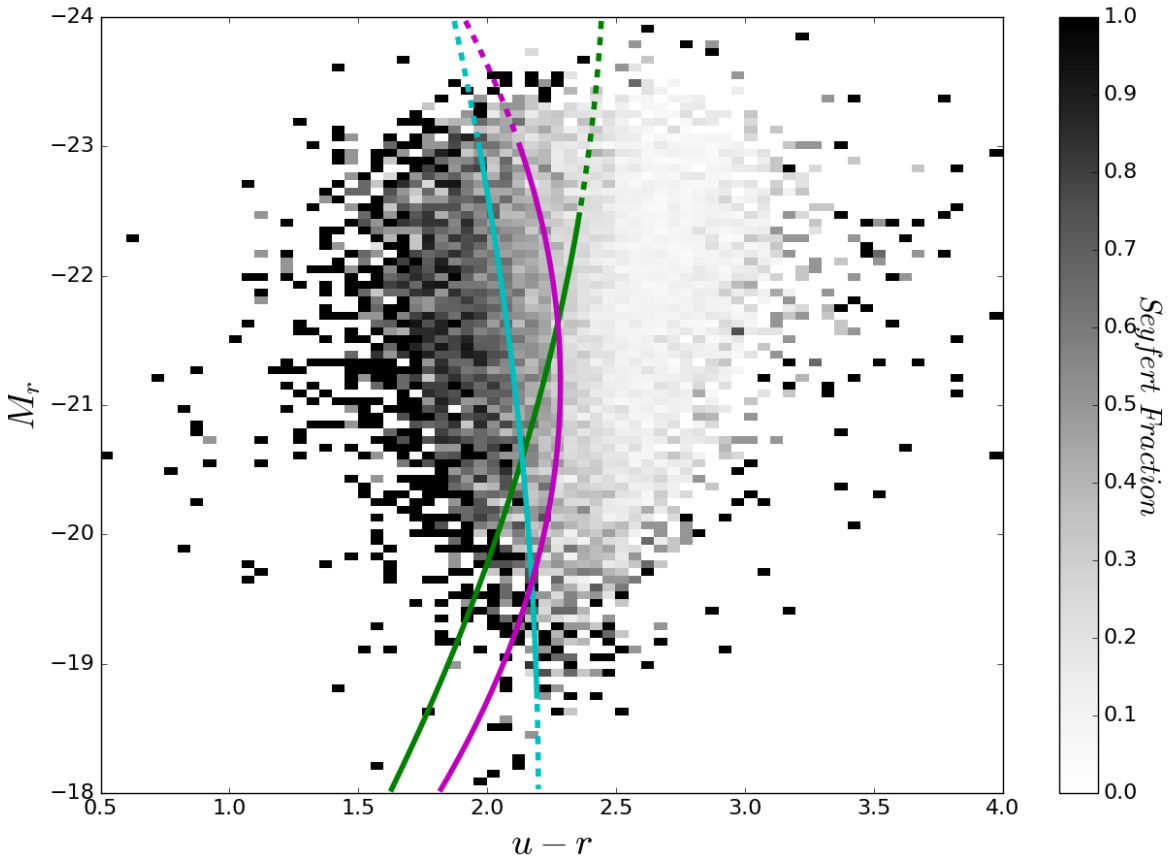

Figure 14: This diagram shows the fraction of Portsmouth identified AGN galaxies (Seyfert or LINER) that are Seyferts. The high Seyfert fractions surrounding the main distribution are bins containing only a few galaxies. Once again, the overlaid dividers correspond to the same color scheme: green is the color divider, cyan is morphological, and magenta is spectroscopic.

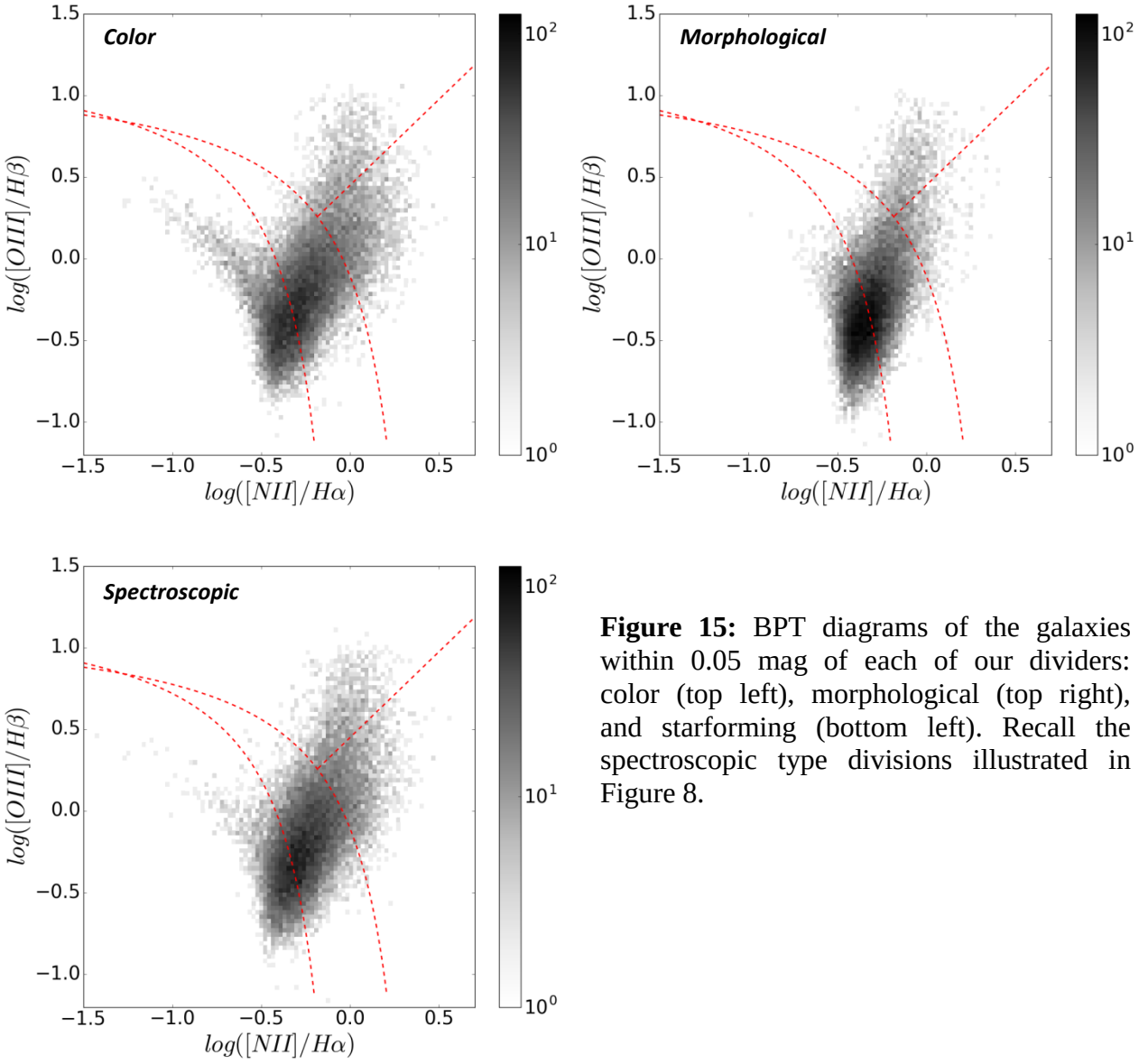

Figure 15: BPT diagrams of the galaxies within 0.05 mag of each of our dividers: color (top left), morphological (top right), and starforming (bottom left). Recall the spectroscopic type divisions illustrated in Figure 8.